Phosphorus, Sulfur, and Silicon and the Related Elements

ISSN: (Print) (Online) Journal homepage: https://www.tandfonline.com/loi/gpss20

Synthesis of novel thiosemicarbazone derivatives as antidiabetic agent with enzyme kinetic studies and antioxidant activity

Fatih Tok, Bahar Küçükal, Nimet Baltaş, Gizem Tatar Yılmaz & Bedia Koçyiğit-Kaymakçıoğlu

To cite this article: Fatih Tok, Bahar Küçükal, Nimet Baltaş, Gizem Tatar Yılmaz & Bedia Koçyiğit-Kaymakçıoğlu (2022) Synthesis of novel thiosemicarbazone derivatives as antidiabetic agent with enzyme kinetic studies and antioxidant activity, Phosphorus, Sulfur, and Silicon and the Related Elements, 197:12, 1284-1294, DOI: 10.1080/10426507.2022.2099857

To link to this article: https://doi.org/10.1080/10426507.2022.2099857

PHOSPHORUS, SULFUR, AND SILICON AND THE RELATED ELEMENTS
2022, VOL. 197, NO. 12, 1284–1294
https://doi.org/10.1080/10426507.2022.2099857

Synthesis of novel thiosemicarbazone derivatives as antidiabetic agent with enzyme kinetic studies and antioxidant activity

Fatih Tok[a], Bahar Küçükal[b], Nimet Baltaş[b], Gizem Tatar Yılmaz[c], and Bedia Koçyiğit-Kaymakçıoğlu[a]

[a]Department of Pharmaceutical Chemistry, Faculty of Pharmacy, Marmara University, Istanbul, Turkey; [b]Department of Chemistry, Faculty of Arts and Sciences, Recep Tayyip Erdoğan University, Rize, Turkey; [c]Department of Biostatistics and Medical Informatics, Faculty of Medicine, Karadeniz Technical University, Trabzon, Turkey

ABSTRACT

Novel thiosemicarbazone derivatives were synthesized *via* condensation reactions between the corresponding thiosemicarbazides and 4-(methylsulfonyl)acetophenone. The chemical structures of all compounds were elucidated by infrared (IR), ^{1}H-NMR and ^{13}C-NMR spectroscopy and mass spectrometry. Antioxidant studies of all compounds were performed by using CUPRAC, FRAP, DPPH methods. 2-{1-[4-(Methylsulfonyl)phenyl]ethylidene}-*N*-phenylhydrazinecarbothioamide (**1**) possessed good antioxidant activity with an SC_{50} value of 15.70 μM which also is higher than standard drug, ascorbic acid. All compounds were evaluated for their antidiabetic properties as α-glycosidase and α-amylase inhibitors. Compound **1** was found to be the most active compound against α-glucosidase and α-amylase with IC_{50} values of 1.58 μM and 3.24 μM, respectively. The enzyme kinetic studies demonstrated that compound **1** has a competitive mode of binding. Furthermore, molecular docking studies have elucidated the binding mechanism at the molecular level by examining the molecular interactions between compound **1** and these enzymes.

ARTICLE HISTORY
Received 4 April 2022
Accepted 6 July 2022

KEYWORDS
Thiosemicarbazones; α-glucosidase; α-amylase; antioxidant; molecular docking

GRAPHICAL ABSTRACT

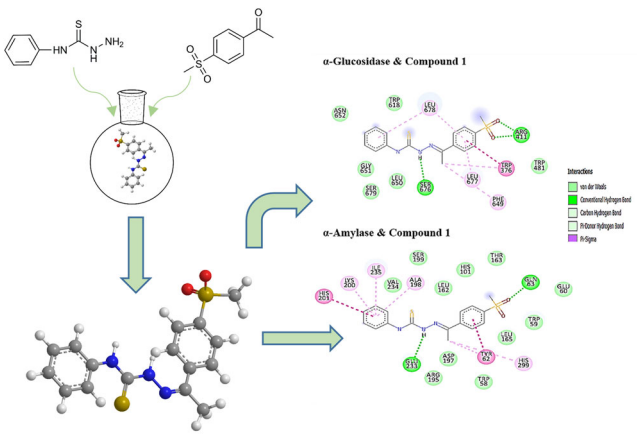

Introduction

Type 2 diabetes mellitus is a complex metabolic disorder which can lead to tissue and organ damages such as nephropathy, retinopathy, and neuropathy.[1] According to the World Health Organization (WHO), 25% of all people between the ages of 30–70 suffer from this metabolic disease.[2] Although there are many antihyperglycemic agents with different mechanisms of action, their uses are limited due to the adverse effects such as hypoglycemia, comorbidities and weight gain.[3] In addition, the efficacy of antidiabetic agents decreases with the long time application.[4] If the antidiabetic agents cannot maintain the glucose level, combined therapy may also be preferred.[5] Hence, there is a continuous need for new effective and selective antidiabetic agents. In the last few years, a new family of drug targets has emerged for the treatment of diabetes that can act by multiple mechanisms.

α-Glucosidase and α-amylase enzymes are valuable strategies for controlling blood glucose levels.[6] While α-amylase catalyzes the hydrolysis of glucose polymers such as starch to oligosaccharides and disaccharides in the mouth and stomach, α-glucosidase hydrolyzes disaccharide molecules to glucose in the small intestine.[7] In order to bind to the active site of the enzymes, both enzyme inhibitors compete with the sugar molecule, thereby effectively reducing the amounts of postprandial glucose.[8–10] Therefore, these

CONTACT Fatih Tok fatih.tok@marmara.edu.tr Department of Pharmaceutical Chemistry, Faculty of Pharmacy, Marmara University, Istanbul 34854, Turkey.
Supplemental data for this article can be accessed online at https://doi.org/10.1080/10426507.2022.2099857.

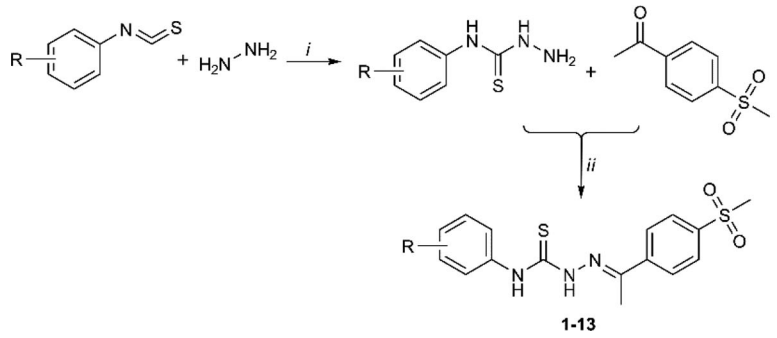

Comp.	R	Comp.	R	Comp.	R
1	H	6	4-OCH_3	11	4-Br
2	4-Cl	7	3,4,5-triOCH_3	12	4-CF_3
3	4-F	8	2,6-diCl	13	2,4,6-triCl
4	4-NO_2	9	2,6-diF		
5	4-CH_3	10	2,4-diCl		

Scheme 1. The synthesis pathway of thiosemicarbazone derivatives. Reagents: (i) hydrazine hydrate, dichloromethane; (ii) ethanol.

mechanisms can be important strategies in the management of blood glucose level in diabetic patients.

The increase in free radicals and reactive oxygen species (ROS) is the cause of various diseases such as metabolic disorders, reperfusion damage, inflammatory diseases, and cellular aging.[11] Antioxidants play an important role in protecting biological systems from reactive oxygen species that can cause damage.[12] Antioxidants are successful in preventing diabetes complications.[13]

Thiosemicarbazones exhibit many biological and pharmacological activities such as antimicrobial, anti-inflammatory, anticancer, antioxidant and antidiabetic properties due to their unique pharmacophore (–NH–C(=S)NH–N=) group.[14,15] Thiosemicarbazones are obtained from the reaction of thiosemicarbazides with aldehydes or ketones and play an important role in medicinal chemistry.[16] The methylsulfonyl unit is an active pharmacophore group found in many drugs. The methylsulfonyl unit is a highly preferred structure in new drug candidate molecules in medicinal chemistry.[17–19] Taking these facts into account, we designed new thiosemicarbazone derivatives bearing methylsulfonyl moiety and screened their α-glucosidase and α-amylase inhibitory potential, enzyme kinetic parameters and their antioxidant properties.

Results and discussion

Chemistry

The thiosemicarbazide compounds were obtained as a result of the nucleophilic addition reaction of hydrazine to substituted isothiocyanates. The thiosemicarbazone derivatives were then obtained with a condensation reaction between 4-(methylsulfonyl)acetophenone and substituted thiosemicarbazides in good to excellent yields (65–85%). The details of all synthesis steps of compounds (**1**–**13**) were outlined in Scheme 1.

In the IR spectra, NH stretching vibrations are located in regions 3111–3363 cm^{-1}. The C–H stretching vibration belonging to the aromatic and aliphatic structure in this molecule were recorded in the region 3001–3086 cm^{-1} and 2833–2974 cm^{-1}, respectively. The calculated wave number at 1587–1595 cm^{-1} was assigned to the stretching vibration mode of imine (C = N). The C = S stretching bands of the thiosemicarbazone group and S = O stretching bands of the sulfone group were observed at 1230–1257 cm^{-1} and 1305–1357 cm^{-1}, respectively. In the ^{1}H-NMR spectra, the methyl protons attached to the imine ($\underline{CH_3}$–C = N) and sulfonyl ($SO_2\underline{CH_3}$) structures resonated at 2.39–2.45 ppm and 3.24–3.26 ppm, respectively. The singlet peaks observed in the range of 10.04 and 11.17 ppm represent the NH protons of thiosemicarbazone derivatives. In the ^{13}C-NMR spectrum, methyl carbons attached to the imine and sulfonyl structures were observed at 14.30–14.91 ppm and 43.42–43.95 ppm, respectively. The imine carbon (C = N) and thiocarbonyl (C = S), which are the characteristic peaks of the thiosemicarbazone structure, were detected at 146.75–148.48 ppm and 176.82–179.83 ppm, respectively.

Compound **1** was chosen as a prototype by identifying NMR spectra. According to ^{1}H-NMR spectra of compound **1**, two peaks at 2.39 ppm and 3.24 ppm attached to imine carbon and sulfonyl moiety were observed as singlets. The two NH signals belonging to thiosemicarbazone appeared as singlets at 10.16 ppm and 10.77 ppm. Aromatic protons of the benzene appeared as a complex multiple in the range of 7.23–8.28 ppm. In the ^{13}C NMR spectrum, compound **1** showed the absorption signals at 14.43 ppm and 43.42 ppm for methyl carbons attached to the imine group and sulfonyl moiety. The imine carbons (C = N) appeared at 146.92 ppm; while the C = S carbon appeared at 177.34 ppm. On the other hand compound **1** in the mass spectra showed a peak at *m/z* 346.4 corresponds to (M–1) ion and a peak at *m/z* 348.3 corresponds to (M + 1) ion.

Biological activity

Antioxidant activity assay

The CUPRAC method of antioxidant capacity measurement is based on the absorbance measurement of the CUPRAC chromophore, Cu(I)–neocuproine (Nc) chelate, formed as a result of the redox reaction of antioxidants with the CUPRAC reagent, bis(neocuproine)copper(II) cation [Cu(II)–Nc], where absorbance is recorded at the maximal light absorption wavelength of 450 nm. The orange-yellow color is due to the Cu(I)–Nc charge–transfer complex formed.[20] With FRAP assay, the sample compounds were tested for their abilities to reduce iron(III) to iron(II) ions, and the absorbance of TPTZ (2,4,6-tripyridyl-1,3,5-s-triazine)–Fe^{2+} complex was measured at 593 nm increasing to higher activity antioxidants. The absorbance measured for the samples was converted to $FeSO_4.7H_2O$ equivalent antioxidant capacity values obtained from the absorbance –[$FeSO_4.7H_2O$] calibration graph, and the μM $FeSO_4.7H_2O$ values are given in Table S1 (Supplemental Materials). Compound **1** was found to be the most effective compound

Table 1. The prediction of physicochemical and pharmacokinetic parameters.

Comp	MW	*n*-ROTB	*n*-ON	*n*-OHNH	cLog P	TPSA	Lipinski	Veber	GI abs.	BBB per.	Bio. Score	PAINS
1	347.46	6	3	2	2.62	111.03	Yes	Yes	High	No	0.55	0 alert
2	381.90	6	3	2	3.13	111.03	Yes	Yes	High	No	0.55	0 alert
3	365.45	6	4	2	3.01	111.03	Yes	Yes	High	No	0.55	0 alert
4	392.45	7	5	2	1.63	156.85	Yes	No	Low	No	0.55	0 alert
5	361.48	6	3	2	2.86	111.03	Yes	Yes	High	No	0.55	0 alert
6	377.48	7	4	2	2.32	120.26	Yes	Yes	High	No	0.55	0 alert
7	437.53	9	6	2	1.73	138.72	Yes	Yes	Low	No	0.55	0 alert
8	416.35	6	3	2	3.63	111.03	Yes	Yes	High	No	0.55	0 alert
9	383.44	6	5	2	3.40	111.03	Yes	Yes	High	No	0.55	0 alert
10	416.35	6	3	2	3.63	111.03	Yes	Yes	High	No	0.55	0 alert
11	426.35	6	3	2	3.25	111.03	Yes	Yes	High	No	0.55	0 alert
12	415.45	7	6	2	3.48	111.03	Yes	Yes	Low	No	0.55	0 alert
13	450.79	6	3	2	4.13	111.03	Yes	Yes	Low	No	0.55	0 alert
Acarbose	645.60	9	19	14	−6.94	321.17	No	No	Low	No	0.17	0 alert

MW: Molecular weight; *n*-ROTB: number of rotatable bonds; *n*-ON: number of hydrogen bond acceptors; *n*-OHNH: number of hydrogen bond donors; cLogP: calculated partition coefficient; TPSA: Topological polar surface area; GI abs.: Gastrointestinal absorption; BBB per.: Blood–brain barrier permeation; Bio. Score: Bioavailability Score; PAINS: Calculations were performed using the Swissadme online server (http://www.swissadme.ch).

in both FRAP and CUPRAC antioxidant assays. In addition to this information, compounds **3**, **7**, **9** and **12** exhibited very good antioxidant activity in both cupric reducing antioxidant activity and ferric reducing antioxidant power assays. The other remaining compounds showed moderately antioxidant properties in this method (Table S1). The DPPH method is based on the fact that the free radical is purple, and that the purple color of DPPH decays in the presence of an antioxidant. The color changed from purple to yellow after reduction, which can be quantified by its decrease of absorbance at wavelength 517 nm. The results were expressed as SC_{50} (μM), which was calculated from the curves by plotting absorbance values, the SC_{50} values representing the concentration of the compound (μM) required to inhibit 50% of the radicals. Because of having the lowest SC_{50} value (15.70 ± 0.13 μM), compound **1** was the best compared to the other synthesized compounds. We can list the molecules whose radical scavenging activity is more effective than ascorbic acid, according to the order of activity as follows: **1** > **7** >Ascorbic acid.

In vitro α-glucosidase inhibition results and kinetic studies

The newly synthesized compounds were examined in terms of their α-glucosidase inhibition potential. The percentage of relative activities versus inhibitor concentrations were plotted separately for each organic molecule. IC_{50} values were determined α-glucosidase and α-amylase inhibitory activity of the synthesized compounds and acarbose were shown in Table S1 (Supplemental Materials). Among the tested compounds, compound **1** showed the most significant α-glucosidase inhibitory activity, with an IC_{50} value of 1.58 ± 0.11 μM (Tables S1 and S2). The α-glucosidase inhibition effectiveness of the compounds, which are more active than acarbose, are listed from the most active molecules to the least active molecules as follows, **1** > **7**>**3** > **12** > **9**>**5**> Acarbose (Tables S1 and S2). To determine the type of enzyme inhibition of **1**, **7**, **3**, **12**, **9**, **5** and acarbose, their α-glucosidase activity was analyzed by Lineweaver–Burk plots using data derived from enzyme assay containing different concentrations of 4-pNPG in the absence or presence of each inhibitor (Figure 1a–g; Table S2). In the presence of **1**, **7**, **3**, **12**, **9**, **5**, K_m value increased and V_{max} value (169.49 mM/min) remained unchanged. From this point of view, the analysis of the Lineweaver–Burk plot indicated that the inhibition type of these compounds was competitive mode (Figure 1a–g). In competitive inhibition, the inhibitor binds to the active site of the enzyme and competes with the substrate. Thus, the inhibitor binds to the active site of the enzyme instead of the substrate, and the K_m value increases. The higher the K_m value, the more the enzyme's affinity for the inhibitor increases. When Table S2 is examined, among the competitive inhibitors, the inhibitor that the enzyme is most interested in is compound **1** with a K_m value of 0.66 mg/mL (Table S2; Figure 1a–g).

In vitro α-amylase inhibition results and kinetic studies

The newly synthesized compounds were examined in terms of their α-amylase inhibition potential. The percentage of relative activities versus inhibitor concentrations were plotted separately for each organic molecule. The α-amylase inhibitory effects of the compounds which are more active than acarbose, are listed from the most active molecules to the least active molecules as follows, **1** > **7**>Acarbose (Tables S1 and S3, Supplemental Materials). The rest of the compounds showed moderate, α-amylase inhibitory activity, within the range of 3.24 ± 0.16–40.20 ± 0.28 μM (Tables S1 and S3). The type of enzyme inhibition of **1**, **7** and acarbosewas determined from their α-amylase activity was by Lineweaver–Burk plots using data derived from enzyme assay containing different concentrations of starch in the absence or presence of each inhibitor (Figure 2a–c; Table S3). In the presence of compounds, **1**, **7** K_m value increased and V_{max} value (285.71 mM/min) remained the same. Looking at the results obtained, the analysis of the Lineweaver–Burk plot indicated that the inhibition type of these compounds was competitive mode (Figure 2a–c). In competitive inhibition, the inhibitor binds to the active site of the enzyme and competes with the substrate. Thus, the inhibitor binds to the active site of the enzyme instead of the substrate, and the K_m value increases. The higher the K_m value, the more the enzyme's affinity for the inhibitor

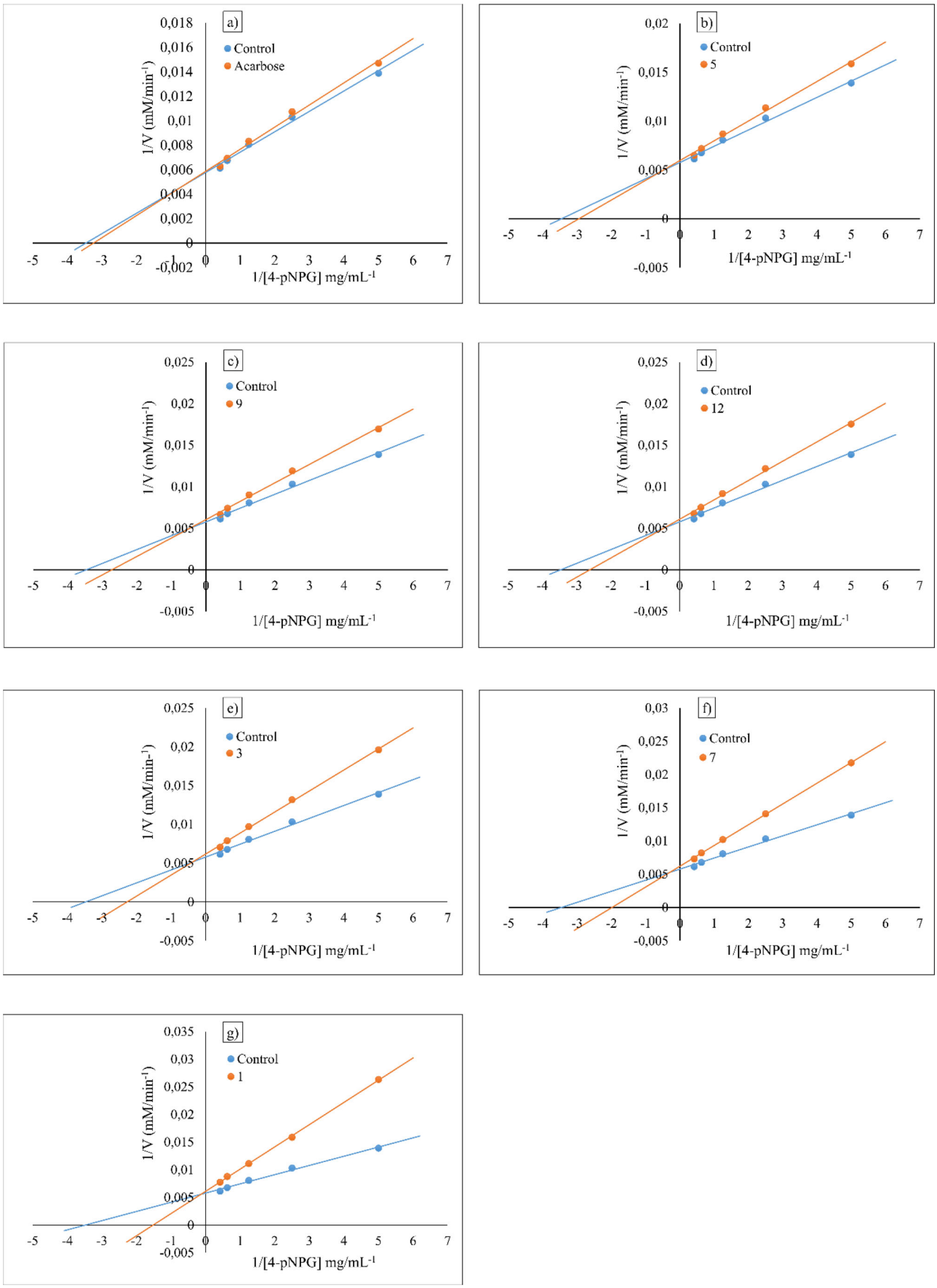

Figure 1. Types of inhibition and Lineweaver–Burk plots of Acarbose **(a)**, compound **5 (b)**, compound **9 (c)**, compound **12 (d)**, compound **3 (e)**, compound **7 (f)**, compound **1 (g)** against the α-glucosidase enzyme.

Table 2. The lowest binding energy values of the synthesized compounds and reference compounds from each docking analysis in the active site of α-amylase and α-glucosidase.

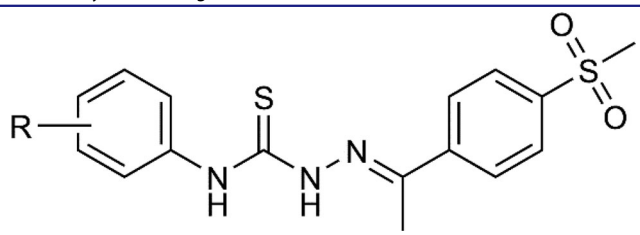

Comp.	*R*	α-amylase binding energy (kcal/mol)	α-glucosidase binding energy (kcal/mol)
1	H	−7.58	−7.39
2	4-Cl	−7.71	−7.19
3	4-F	−7.58	−6.69
4	4-NO_2	−7.56	−6.88
5	4-CH_3	−8.14	−6.90
6	4-OCH_3	−8.14	−6.78
7	3,4,5-triOCH_3	−7.34	−6.55
8	2,6-diCl	−8.35	−7.38
9	2,6-diF	−7.55	−6.64
10	2,4-diCl	−8.32	−7.09
11	4-Br	−7.92	−6.96
12	4-CF_3	−7.37	−6.59
13	2,4,6-triCl	−7.91	−7.41
Acarbose (Reference compound)		−6.30	−4.66

increases. When Table S3 is examined, among the competitive inhibitors, the inhibitor that the enzyme is most interested in is compound **1** with a K_m value of 0.95 mg/mL, as in the glucosidase enzyme inhibition assay and kinetic study result (Table S3; Figure 2a–c).

The prediction of physicochemical and pharmacokinetic profiles of compounds

The physicochemical and pharmacokinetic properties of all compounds were evaluated by *in silico* methods. Drug-likeness properties such as the Lipinski and Veber rule were also calculated. According to the results, all compounds complied with Lipinski and Veber rule (only compound **4** violated Veber rule). To obtain good antidiabetic activity, the compound must pass through the gastrointestinal membranes. Therefore the majority of compounds had passive absorption by the gastrointestinal tract. On the other hand, it was predicted that the blood–brain barrier crossing of all the compounds was low, so the possibility of toxic or other unwanted adverse effects decreased in the central nervous system. The bioavailability score indicates the probability that a compound has at least 10% oral bioavailability or measurable Caco-2 permeability in the rat. The bioavailability score of all compounds was the accepted value of 0.55 (Table 1).

Bioavailability Radar is an important parameter for rapid assessment of drug-likeness. This parameter is a diagram containing six physicochemical properties such as lipophilicity, size, polarity, solubility, flexibility, and saturation.[21] An ideal drug molecule is depicted in the pink area inside the hexagon containing these physicochemical properties. It was found that compounds are slightly outside the pink area on one side, due to the inconformity of saturation. Compound **4** carrying polar nitro substituent was also slightly outside the pink area on two side due to the inconformities of saturation and polarity. The other compounds exhibited good bioavailability radar. The bioavailability radar of all compounds was given in Figure S1 (Supplemental Materials). The bioavailability radar showed the prediction of a compound to have at least 10% oral bioavailability. Therefore all synthesized compounds were more easily orally absorbed than acarbose according to bioavailability results.

In silico molecular docking analysis for α-amylase and α-glucosidase enzyme

Molecular docking is one of the most frequently used methods in structure-based drug design because of its ability to predict the binding conformation and affinity of small-molecule ligands within the appropriate target enzyme binding site with considerable accuracy. In light of this information, all newly synthesized compounds revealed better binding affinity against target enzymes than the reference compound acarbose (see Table 2). Especially, compounds **1** and **7** showed potent inhibitory effects against α-amylase and α-glucosidase enzymes *in vitro* and *in silico* studies. The potent compound **1** displayed strong hydrogen bond interactions with Gln63 (1.71 Å), Glu233 (2.43 Å), π–π stacked bond with Tyr62, π–π T-shaped bond with His201, π-alkyl bond with His299, Ala198, Lys200 and Ile235 in the α-amylase binding site. At the same time, the other potent compound **7** formed hydrogen bond interactions with Asn150, Asn152, Ile235, Glu240, Val234, Tyr151 residues of α-amylase. Besides, this compound has interacted π-sigma bond with Ile235, π-alkyl bond with Lys200 in the α-amylase active site (see Figure S2).

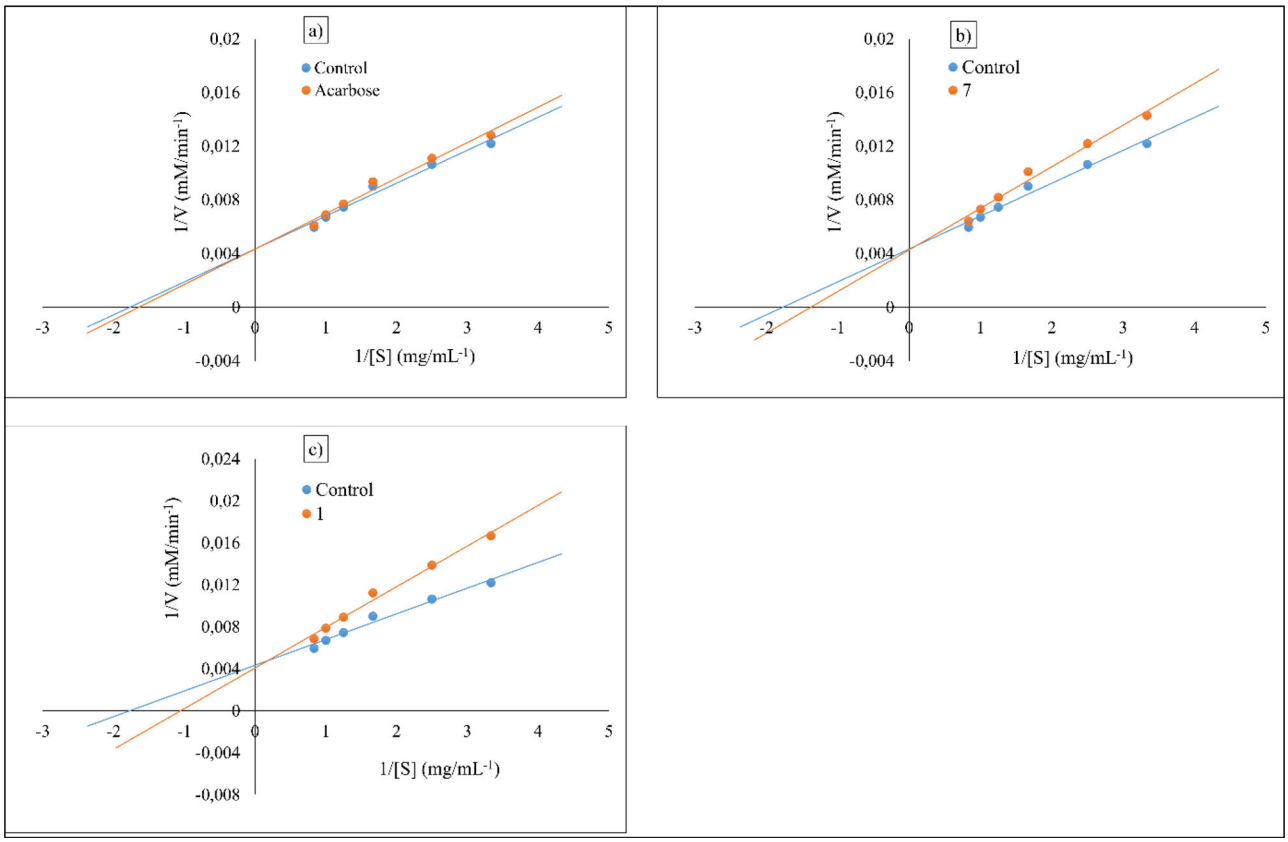

Figure 2. Types of inhibition and Lineweaver–Burk plots of Acarbose **(a)**, compound **1** **(b)**, compound **7** **(c)** against the α-amylase enzyme.

Furthermore, compounds **1** and **7**, which show a good inhibitory effect against α-glucosidase both *in vitro* and *in silico* studies, it was observed that bound with Arg411, Ser676, Asp404, and Asn616 residues of α-glucosidase with hydrogen bonds (see Figure S2). In addition, compound **1** exhibited four π-alkyl bonds with Trp376, Phe649, Leu678, Leu677 residues of α-glucosidase. Also, compound **7** formed six π-alkyl bonds with Trp376, Trp481, Leu650, Leu677, Phe649, Met519 (see Figure S2).

Materials and methods

Chemistry

All chemicals and reagents were purchased from Sigma-Aldrich (St.Louis, MO, USA) or Merck Chemical Company (Darmstadt, Germany) and used without further purification. Melting points were determined on a Stuart SMP II digital melting point apparatus (Cole-Parmer Ltd. Staffordshire, UK) and are uncorrected. The IR spectra were recorded using a Shimadzu FTIR 8400S spectrometry. The NMR spectra were taken on a Bruker Avance Neo 400 MHz (Palo Alto, CA, USA), operating at 400 MHz (^{1}H-NMR), and 100 MHz (^{13}C-NMR) in DMSO-d_6. Chemical shifts (δ) were expressed in parts per million relative to tetramethylsilane used as the internal reference. Mass spectra were verified on an APCI-MS (Advion, New York, USA) using the APCI method. The Supplemental Materials contains sample ^{1}H and ^{13}C NMR, IR and mass spectra of the products 1–13 (Figures S3–S54).

General procedure for the synthesis of the thiosemicarbazide derivatives

Hydrazine monohydrate (1 mmol) was taken in dichloromethane (5 mL). A solution of substituted phenylisothiocyanate (1 mmol) in dichloromethane (5 mL) was added dropwise to the hydrazine hydrate solution followed by stirring of the reaction mixture for 8 h at room temperature.[22]

General procedure for the synthesis of the thiosemicarbazone derivatives (1–13)

N-phenylhydrazinecarbothioamide (1 mmol) and 1-[4-(methylsulfonyl)phenyl]ethanone (1 mmol) were dissolved in ethanol (20 mL). The mixture was refluxed for 10–12 h. After TLC control, the excess solvent was evaporated under vacuum. The residue was recrystallized from methanol.[23]

2-{1-[4-(Methylsulfonyl)phenyl]ethylidene}-N-phenylhydrazinecarbothioamide (1)

Yield: 81%; m.p. 203.9–204.5 °C. IR (ν, cm^{-1}): 3355, 3275, 3171 (N–H), 3022 (aromatic C–H), 2887 (aliphatic C–H), 1587 (C = N), 1351 (SO_2), 1251 (C = S). ^{1}H-NMR (400 MHz, DMSO-d_6, ppm): δ 2.39 (s, 3H, =CCH_3), 3.24 (s, 3H, SO_2CH_3), 7.23–8.28 (m, 9H, Ar–H), 10.16 (s, 1H, NH), 10.77 (s, 1H, NH). ^{13}C-NMR (125 MHz, DMSO-d_6, ppm): δ 14.43 (CH_3), 43.42 (SO_2CH_3), 125.56, 126.10, 126.78, 127.65, 128.10, 139.08, 140.85, 142.31, 146.92 (C = N), 177.34

(C = S). MS (APCI): $C_{16}H_{17}N_3O_2S_2$; calculated $m/z = 347.5$ $[M^+]$, found $m/z = 348.3$ $[M + H]^+$.

N-(4-Chlorophenyl)-2-{1-[4-(methylsulfonyl)phenyl]ethylidene}hydrazinecarbothioamide (2)

Yield: 85%; m.p. 237.2–237.8 °C. IR (ν, cm^{-1}): 3354, 3263, 3167 (N–H), 3076 (aromatic C–H), 2918 (aliphatic C–H), 1591 (C = N), 1307 (SO_2), 1240 (C = S). ^{1}H-NMR (400 MHz, DMSO-d_6, ppm): δ 2.42 (s, 3H, =CCH_3), 3.24 (s, 3H, SO_2CH_3), 7.43–8.41 (m, 8H, Ar–H), 10.19 (s, 1H, NH), 10.87 (s, 1H, NH). ^{13}C-NMR (125 MHz, DMSO-d_6, ppm): δ 14.51 (CH_3), 43.45 (SO_2CH_3), 126.78, 127.69, 127.75, 127.99, 129.55, 138.07, 140.93, 142.25, 147.36 (C = N), 177.38 (C = S). MS (APCI): $C_{16}H_{16}ClN_3O_2S_2$; calculated $m/z = 381.9$ $[M^+]$, found $m/z = 382.5$ $[M + H]^+$.

N-(4-Fluorophenyl)-2-{1-[4-(methylsulfonyl)phenyl]ethylidene}hydrazinecarbothioamide (3)

Yield: 85%; m.p. 233.8–234.2 °C. IR (ν, cm^{-1}): 3363, 3294, 3179 (N–H), 3012 (aromatic C–H), 2918 (aliphatic C–H), 1587 (C = N), 1357 (SO_2), 1257 (C = S). ^{1}H-NMR (500 MHz, DMSO-d_6, ppm): δ 2.42 (s, 3H, =CCH_3), 3.26 (s, 3H, SO_2CH_3), 7.24 (t, 2H, Ar–H), 7.53 (m, 2H, Ar–H), 7.94 (t, 2H, Ar–H), 8.27 (t, 2H, Ar–H), 10.16 (s, 1H, NH), 10.82 (s, 1H, NH). ^{13}C-NMR (125 MHz, DMSO-d_6, ppm): δ 14.71 (CH_3), 43.90 (SO_2CH_3), 115.35, 127.26, 128.16, 128.99,135.96, 141.44, 142.71, 147.56 (C = N), 159.33, 161.26, 178.23 (C = S). MS (APCI): $C_{16}H_{16}FN_3O_2S_2$; calculated $m/z = 365.4$ $[M^+]$, found $m/z = 366.1$ $[M + H]^+$.

2-{1-[4-(Methylsulfonyl)phenyl]ethylidene}-N-(4-nitrophenyl)hydrazinecarbothioamide (4)

Yield: 75%; m.p. 243.1–243.4 °C. IR (ν, cm^{-1}): 3352, 3271, 3128 (N–H), 3026 (aromatic C–H), 2929 (aliphatic C–H), 1595 (C = N), 1323 (SO_2), 1253 (C = S). ^{1}H-NMR (400 MHz, DMSO-d_6, ppm): δ 2.45 (s, 3H, =CCH_3), 3.25 (s, 3H, SO_2CH_3), 7.94 (d, $J = 8.2$ Hz, 2H, Ar–H), 8.02 (d, $J = 8.2$ Hz, 2H, Ar–H), 8.24 (m, 4H, Ar–H), 10.47 (s, 1H, NH), 11.17 (s, 1H, NH). ^{13}C-NMR (125 MHz, DMSO-d_6, ppm): δ 14.80 (CH_3), 43.44 (SO_2CH_3), 123.73, 124.74, 126.84, 127.80, 141.12, 142.16, 143.63, 145.32, 148.48 (C = N), 176.82 (C = S). MS (APCI): $C_{16}H_{16}N_4O_4S_2$; calculated $m/z = 392.5$ $[M^+]$, found $m/z = 393.1$ $[M + H]^+$.

2-{1-[4-(Methylsulfonyl)phenyl]ethylidene}-N-p-tolylhydrazinecarbothioamide (5)

Yield: 77%; m.p. 238.8–239.1 °C. IR (ν, cm^{-1}): 3342, 3282, 3119 (N–H), 3010 (aromatic C–H), 2916 (aliphatic C–H), 1589 (C = N), 1313 (SO_2), 1234 (C = S). ^{1}H-NMR (400 MHz, DMSO-d_6, ppm): δ 2.32 (s, 3H, CH_3), 2.41 (s, 3H, =CCH_3), 3.24 (s, 3H, SO_2CH_3), 7.17 (d, $J = 8.0$ Hz, 2H, Ar–H), 7.39 (d, $J = 8.0$ Hz, 2H, Ar–H), 7.90 (d, $J = 8.4$ Hz, 2H, Ar–H), 8.26 (d, $J = 8.4$ Hz, 2H, Ar–H), 10.09 (s, 1H, NH), 10.71 (s, 1H, NH). ^{13}C-NMR (125 MHz, DMSO-d_6, ppm): δ 14.38 (CH_3), 20.59, 43.46 (SO_2CH_3), 126.01, 126.86, 127.63, 128.56, 134.74, 136.51, 140.82, 142.33, 146.75 (C = N), 177.37 (C = S). MS (APCI): $C_{17}H_{19}N_3O_2S_2$; calculated $m/z = 361.5$ $[M^+]$, found $m/z = 362.1$ $[M + H]^+$.

N-(4-Methoxyphenyl)-2-{1-[4-(methylsulfonyl)phenyl]ethylidene}hydrazinecarbothioamide (6)

Yield: 72%; m.p. 227.5–227.8 °C. IR (ν, cm^{-1}): 3312, 3202, 3111 (N–H), 3010 (aromatic C–H), 2833 (aliphatic C–H), 1587 (C = N), 1318 (SO_2), 1236 (C = S). ^{1}H-NMR (500 MHz, DMSO-d_6, ppm): δ 2.42 (s, 3H, =CCH_3), 3.25 (s, 3H, SO_2CH_3), 3.77 (s, 3H, OCH_3), 6.94 (d, $J = 8.8$ Hz, 2H, Ar–H), 7.38 (d, $J = 8.8$ Hz, 2H, Ar–H), 7.91 (d, $J = 8.5$ Hz, 2H, Ar–H), 8.27 (d, $J = 8.5$ Hz, 2H, Ar–H), 10.07 (s, 1H, NH), 10.69 (s, 1H, NH). ^{13}C-NMR (125 MHz, DMSO-d_6, ppm): δ 14.82 (CH_3), 43.95 (SO_2CH_3), 55.73, 113.79, 127.26, 128.29, 132.46, 141.27, 142.83, 147.09 (C = N), 157.59, 178.17 (C = S). MS (APCI): $C_{17}H_{19}N_3O_3S_2$; calculated $m/z = 377.5$ $[M^+]$, found $m/z = 378.3$ $[M + H]^+$.

2-{1-[4-(Methylsulfonyl)phenyl]ethylidene}-N-(3,4,5-trimethoxyphenyl)hydrazinecarbothioamide (7)

Yield: 65%; m.p. 215.3–215.7 °C. IR (ν, cm^{-1}): 3279, 3132 (N–H), 3047 (aromatic C–H), 2918 (aliphatic C–H), 1593 (C = N), 1310 (SO_2), 1230 (C = S). ^{1}H-NMR (400 MHz, DMSO-d_6, ppm): δ 2.42 (s, 3H, =CCH_3), 3.25 (s, 3H, SO_2CH_3), 3.66 (s, 3H, OCH_3), 3.77 (s, 6H, $2OCH_3$), 6.97 (d, $J = 7.6$ Hz, 2H, Ar–H), 7.94 (m, 2H, Ar–H), 8.22 (s, 2H, Ar–H), 10.04 (s, 1H, NH), 10.77 (s, 1H, NH). ^{13}C-NMR (125 MHz, DMSO-d_6, ppm): δ 14.53 (CH_3), 43.46 (SO_2CH_3), 55.95, 60.14, 103.74, 126.85, 127.70, 134.85, 135.17, 140.90, 142.32, 147.07 (C = N), 152.24, 177.04 (C = S). MS (APCI): $C_{19}H_{23}N_3O_5S_2$; calculated $m/z = 437.5$ $[M^+]$, found $m/z = 438.3$ $[M + H]^+$.

N-(2,6-Dichlorophenyl)-2-{1-[4-(methylsulfonyl)phenyl]ethylidene}hydrazinecarbothioamide (8)

Yield: 72%; m.p. 232.5–232.9 °C. IR (ν, cm^{-1}): 3257 (N–H), 3012 (aromatic C–H), 2939 (aliphatic C–H), 1591 (C = N), 1305 (SO_2), 1251 (C = S). ^{1}H-NMR (500 MHz, DMSO-d_6, ppm): δ 2.42 (s, 3H, =CCH_3), 3.25 (s, 3H, SO_2CH_3), 7.37 (m, 2H, Ar–H), 7.55 (d, $J = 8.0$ Hz, 2H, Ar–H), 7.90 (m, 2H, Ar–H), 8.24 (m, 2H, Ar–H), 10.14 (s, 1H, NH), 11.02 (s, 1H, NH). ^{13}C-NMR (125 MHz, DMSO-d_6, ppm): δ 14.30 (CH_3), 43.46 (SO_2CH_3), 126.72, 127.65, 128.29, 129.35, 135.08, 140.86, 142.19, 146.77, 147.25 (C = N), 178.46 (C = S). MS (APCI): $C_{16}H_{15}Cl_2N_3O_2S_2$; calculated $m/z = 416.3$ $[M^+]$, found $m/z = 417.1$ $[M + H]^+$.

N-(2,6-Difluorophenyl)-2-{1-[4-(methylsulfonyl)phenyl]ethylidene}hydrazinecarbothioamide (9)

Yield: 70%; m.p. 209.1–209.7 °C. IR (ν, cm^{-1}): 3333, 3259, 3165 (N–H), 3022 (aromatic C–H), 2941 (aliphatic C–H), 1591 (C = N), 1305 (SO_2), 1236 (C = S). ^{1}H-NMR (500 MHz, DMSO-d_6, ppm): δ 2.42 (s, 3H, =CCH_3), 3.25 (s, 3H, SO_2CH_3), 7.19 (t, 2H, Ar–H), 7.43 (m, 1H, Ar–H), 7.91 (m, 2H, Ar–H), 8.24 (m, 2H, Ar–H), 10.12 (s, 1H, NH), 11.06 (s, 1H, NH). ^{13}C-NMR (125 MHz, DMSO-d_6, ppm): δ

14.91 (CH_3), 43.90 (SO_2CH_3), 112.11, 117.46, 127.23, 127.97, 129.52, 141.44, 142.62, 147.89 (C = N), 158.44, 160.42, 179.83 (C = S). MS (APCI): $C_{16}H_{15}F_2N_3O_2S_2$; calculated $m/z = 383.4$ $[M^+]$, found $m/z = 384.8$ $[M+H]^+$.

N-(2,4-Dichlorophenyl)-2-{1-[4-(methylsulfonyl)phenyl]ethylidene}hydrazinecarbothioamide (10)

Yield: 77%; m.p. 217.7–217.9 °C. IR (ν, cm^{-1}): 3289, 3169 (N–H), 3012 (aromatic C–H), 2887 (aliphatic C–H), 1593 (C = N), 1305 (SO_2), 1249 (C = S). ^{1}H-NMR (500 MHz, DMSO-d_6, ppm): δ 2.42 (s, 3H, =CCH_3), 3.25 (s, 3H, SO_2CH_3), 7.49 (d, $J = 2.5$ Hz, 1H, Ar–H), 7.73 (m, 2H, Ar–H), 7.94 (t, 2H, Ar–H), 8.24 (m, 2H, Ar–H), 10.12 (s, 1H, NH), 11.06 (s, 1H, NH). ^{13}C-NMR (125 MHz, DMSO-d_6, ppm): δ 14.71 (CH_3), 43.89 (SO_2CH_3), 127.32, 127.80, 127.98, 128.09, 129.27, 131.59, 136.41, 141.44, 142.66, 147.72 (C = N), 178.42 (C = S). MS (APCI): $C_{16}H_{15}Cl_2N_3O_2S_2$; calculated $m/z = 416.3$ $[M^+]$, found $m/z = 417.0$ $[M+H]^+$.

N-(4-Bromophenyl)-2-{1-[4-(methylsulfonyl)phenyl]ethylidene}hydrazinecarbothioamide (11)

Yield: 80%; m.p. 222.2–222.8 °C. IR (ν, cm^{-1}): 3354, 3271 (N–H), 3086 (aromatic C–H), 2974 (aliphatic C–H), 1591 (C = N), 1311 (SO_2), 1255 (C = S). ^{1}H-NMR (400 MHz, DMSO-d_6, ppm): δ 2.42 (s, 3H, =CCH_3), 3.25 (s, 3H, SO_2CH_3), 7.54 (m, 4H, Ar–H), 7.91 (d, $J = 8.4$ Hz, 2H, Ar–H), 8.25 (d, $J = 8.4$ Hz, 2H, Ar–H), 10.18 (s, 1H, NH), 10.88 (s, 1H, NH). ^{13}C-NMR (125 MHz, DMSO-d_6, ppm): δ 14.52 (CH_3), 43.45 (SO_2CH_3), 117.79, 126.77, 127.69, 128.04, 130.91, 138.50, 140.93, 142.24, 147.39 (C = N), 177.29 (C = S). MS (APCI): $C_{16}H_{16}BrN_3O_2S_2$; calculated $m/z = 426.4$ $[M^+]$, found $m/z = 425.1$ $[M–H]^+$.

2-{1-[4-(Methylsulfonyl)phenyl]ethylidene}-N-(4-(trifluoromethyl)phenyl)hydrazinecarbothioamide(12)

Yield: 82%; m.p. 245.6–245.8 °C. IR (ν, cm^{-1}): 3360, 3279 (N–H), 3047 (aromatic C–H), 2874 (aliphatic C–H), 1589 (C = N), 1313 (SO_2), 1253 (C = S). ^{1}H-NMR (500 MHz, DMSO-d_6, ppm): δ 2.42 (s, 3H, =CCH_3), 3.25 (s, 3H, SO_2CH_3), 7.74 (d, $J = 8.5$ Hz, 2H, Ar–H), 7.87 (d, $J = 8.5$ Hz, 2H, Ar–H), 7.94 (m, 2H, Ar–H), 8.24 (t,2H, Ar–H), 10.34 (s, 1H, NH), 11.01 (s, 1H, NH). ^{13}C-NMR (125 MHz, DMSO-d_6, ppm): δ 14.71 (CH_3), 43.92 (SO_2CH_3), 123.70, 125.61, 125.86, 126.32, 127.30, 128.24, 141.50, 142.70, 143.29, 147.73 (C = N), 177.68 (C = S). MS (APCI): $C_{17}H_{16}F_3N_3O_2S_2$; calculated $m/z = 415.5$ $[M^+]$, found $m/z = 414.4$ $[M–H]^+$.

2-{1-[4-(Methylsulfonyl)phenyl]ethylidene}-N-(2,4,6-trichlorophenyl)hydrazinecarbothioamide (13)

Yield: 67%; m.p. 240.0–240.4 °C. IR (ν, cm^{-1}): 3254, 3167 (N–H), 3001 (aromatic C–H), 2918 (aliphatic C–H), 1587 (C = N), 1307 (SO_2), 1238 (C = S). ^{1}H-NMR (400 MHz, DMSO-d_6, ppm): δ 2.42 (s, 3H, =CCH_3), 3.25 (s, 3H, SO_2CH_3), 7.80 (s, 1H, Ar–H), 7.91 (m, 3H, Ar–H), 8.24 (m,2H, Ar–H), 10.11 (s, 1H, NH), 11.05 (s, 1H, NH). ^{13}C-NMR (125 MHz, DMSO-d_6, ppm): δ 14.46 (CH_3), 43.48 (SO_2CH_3), 126.81, 127.71, 128.09, 132.63, 134.81, 136.00, 140.94, 142.18, 147.22 (C = N), 178.46 (C = S). MS (APCI): $C_{16}H_{14}Cl_3N_3O_2S_2$; calculated $m/z = 450.8$ $[M^+]$, found $m/z = 452.1$ $[M+H]^+$.

Biological activity

Antioxidant activity

Antioxidant activities and radical scavenging properties of the synthesized compounds were clarified using various *in vitro* antioxidant assays including CUPric reducing antioxidant capacity (CUPRAC),[24] ferric reducing antioxidant power (FRAP) assay,[25,26] and DPPH (1,1-diphenyl-2-picrylhydrazyl) assay.[26,27]

Cupric reducing antioxidant capacity (CUPRAC) assay

The cupric reducing antioxidant capacity of the synthesized compounds was determined according to the literature.[24] Trolox® (Sigma Chemical Co, USA) was tested under the same conditions as a standard antioxidant compound and the standard curve was linear between 8 mg/mL and 0.03125 mg/mL (r^2=0.9987). CUPRAC values were expressed as mM Trolox equivalent of 1 mg synthesized compound.

Ferric reducing antioxidant power (FRAP) assay

The Ferric Reducing Antioxidant Power (FRAP) assay was used to determine total antioxidant capacity. The FRAPreagent used was made by mixing 25 mL acetate buffer (300 mM, pH 3.6), with 2.5 mL of 10 mM TPTZ solution in 40 mM HCl and 2.5 mL of 20 mM $FeCl_3.6H_2O$ solution.[25,26] $FeSO_4.7H_2O$ was used as a positive control to construct a reference curve at six different concentrations (15.63–31.25–62.5–125–250–500–1000 μM, r^2=0.999). FRAP values were expressed as mM $FeSO_4.7H_2O$ equivalent per milligram of the compound, calculated as the $FeSO_4.7H_2O$ concentration from the graph corresponding to the absorbance observed with the sample.

DPPH-free radical scavenging assay

The 1,1-diphenyl-2-picrylhydrazyl (DPPH) radical has been used widely in the model system to investigate the scavenging activities of several synthesized and natural compounds. The DPPH radical scavenging activity of the synthesized compounds was measured using the method of Brand–Williams.[26,27] Radical scavenging activity was measured by using ascorbic acid as standard and all values are expressed as SC_{50} (μg compound per mL), the concentration of the samples that causes 50% scavenging of DPPH radical. The DPPH radical stock solution was prepared fresh daily. All determinations were carried out three times.

In vitro α-glucosidase inhibition assay and kinetic studies

α-Glucosidase from *Saccharomyces cerevisiae* inhibition assay was determined spectrophotometrically.[28,29] Acarbose was used as a standard inhibitor. The IC_{50} value was determined as the concentration of compound that gives 50% inhibition of maximal activity. The α-glucosidase inhibition percentage was calculated as follows:

$$\alpha - glucosidase\ inhibition\ (\%) = [(Acontrol - Asample)/Acontrol]\ \times 100$$

where $A_{control}$ is the activity of enzyme without compound/standard and A_{sample} is the activity of the enzyme with compound/standard at different concentrations.

In the perform α-glucosidase kinetic studies,[30] compounds **1**, **3**, **7**, **9**, **12** and acarbose were evaluated to determine the type of α-glucosidase inhibition. In the test tubes, the substrate concentrations were 0.20, 0.40, 0.80, 1.6 and 2.4 mg/mL in the buffer (pH 6.8) containing enzyme solution (20 U/mL), with (**1**, **3**, **7**, **9**, **12** and acarbose) or without inhibitor solutions.The Lineweaver–Burk graphs were obtained and inhibition patterns were evaluated.

In vitro α-amylase inhibitory activity and kinetic studies

The inhibition of α-amylase activity was performed according to a previously described methods.[29,31] Acarbose was used as a standard inhibitor. The α-amylase inhibition percentage was calculated as follows:

$$\alpha - amylase\ inhibition\ (\%) = [(Acontrol - Asample)/Acontrol]\ \times 100$$

where $A_{control}$ is the activity of enzyme without compound/standard and A_{sample} is the activity of the enzyme with compound/standard at different concentrations. The concentration of the inhibitor required for inhibiting 50% of the enzyme activity under the assay conditions was defined as the IC_{50}.

Compounds **1**, **7** and acarbose were further studied to determine the type of α-amylase inhibition and enzyme kinetic parameters. In the reaction media, the substrate concentrations were 0.30, 0.40, 0.60, 0.80 and 1.2 mg/mL in the buffer (pH 6.9) containing enzyme solution, with (**1**, **7** and acarbose) or without inhibitor solutions.The Lineweaver–Burke graphs[30] were obtained, K_m and V_{max} values were calculated, and inhibition patterns were evaluated.

Prediction of physicochemical and pharmacokinetic parameters

The physicochemical, pharmacokinetic profiles and bioavailability radar of synthesized compounds were determined by using the SwissAdme online server (http://www.swissadme.ch/).

Molecular docking

In this study, molecular docking analysis was performed with AutoDock 4.2.[32] Lamarckian Genetic Algorithm (LGA) was used for the conformational search step in the binding site of the target structures of the flexible ligand (for 100 independent runs of each ligand). The other docking search parameters were preferred with their default values. The three-dimensional (3D) crystal structures of target enzymes, α-amylase (PDB ID: 4W93, resolution:1.35 Å) and α-glucosidase (PDB ID: 5NN4, resolution: 1.8 Å) were accessed from the protein database. The active site of α-amylase and α-glucosidase enzymes was determined by the AGFR1.2[33] program according to the location of the binding site of the crystallized ligands and the active residues at the binding site. The enzyme–ligand complexes with the best docking score were two-dimensional (2D) visualized and analyzed (non-covalent interaction analysis) using Discovery Studio Visualizer software.[34]

Conclusion

The aim of this study was to obtain novel compounds that inhibit α-glucosidase and α-amylase enzymes and also have antioxidant activity against diabetes mellitus. From this point of view, compound **1** and compound **7** synthesized in this study displayed a better inhibitory effect against α-glucosidase and α-amylase than acarbose *in vitro* and *in silico* studies. *In silico* molecular docking analysis also showed that these active compounds formed significant interactions in the active site of the target enzyme, and these interactions could play an important role in increasing the binding affinity. Compound **1** and compound **7** also showed higher antioxidant activity than ascorbic acid. Based on the results, the present study revealed a new class of α-glucosidase and α-amylase inhibitors which can be useful for the design of new drug candidates for the treatment of diabetes.

Acknowledgments

The numerical calculations reported in this abstract were performed at The Scientific and Technological Research Council of Turkey (TUBITAK) ULAKBIM High Performance and Grid Computing Center (TRUBA resources).

Disclosure statement

The authors declare that they have no confict of interest.

ORCID

Fatih Tok http://orcid.org/0000-0002-4569-008X

References

[1] Tavaf, Z.; Dangolani, S. K.; Yousefi, R.; Panahi, F.; Shahsavani, M. B.; Khalafi-Nezhad, A. Synthesis of New Curcumin Derivatives as İnfluential Antidiabetic A-Glucosidase and A-Amylase İnhibitors with Anti-Oxidant Activity. *Carbohydr. Res.* **2020**, *494*, 108069–108010. DOI: 10.1016/j.carres.2020.108069.

[2] Kotkar, G. D.; Clement, M. J.; Tilve, A. S.; Shirsat, R. N.; Nadkarni, V. S.; Ghadi, S. C.; Tilve, S. G. Synthesis, Activity and *İn Silico* Studies of Novel Bisindolylmethanes from Xylochemical 5-Hydroxymethylfurfural as Antidiabetic Agents.

J. Mol. Struct. **2022**, *1254*, 132370–132310. DOI: 10.1016/j.molstruc.2022.132370.

[3] Chaudhury, A.; Duvoor, C.; Reddy Dendi, V. S.; Kraleti, S.; Chada, A.; Ravilla, R.; Marco, A.; Shekhawat, N. S.; Montales, M. T.; Kuriakose, K.; et al. Clinical Review of Antidiabetic Drugs: Implications for Type 2 Diabetes Mellitus Management. *Front. Endocrinol. (Lausanne)* **2017**, *8*, 6–12. DOI: 10.3389/fendo.2017.00006.

[4] Zhu, Y.; Zhao, J.; Luo, L.; Gao, Y.; Bao, H.; Li, P.; Zhang, H. Research Progress of Indole Compounds with Potential Antidiabetic Activity. *Eur. J. Med. Chem.* **2021**, *223*, 113665–113635. DOI: 10.1016/j.ejmech.2021.113665.

[5] Prashantha Kumar, B. R.; Baig, N. R.; Sudhir, S.; Kar, K.; Kiranmai, M.; Pankaj, M.; Joghee, N. M. Discovery of Novel Glitazones İncorporated with Phenylalanine and Tyrosine: Synthesis, Antidiabetic Activity and Structure–Activity Relationships. *Bioorg. Chem.* **2012**, *45*, 12–28. DOI: 10.1016/j.bioorg.2012.08.002.

[6] Li, X.; Bai, Y.; Jin, Z.; Svensson, B. Food-Derived Non-Phenolic α-Amylase and α-Glucosidase İnhibitors for Controlling Starch Digestion Rate and Guiding Diabetes-Friendly Recipes. *LWT – Food Sci. Technol.* **2022**, *153*, 112455–112457. DOI: 10.1016/j.lwt.2021.112455.

[7] Taslimi, P.; Gulçin, İ. Antidiabetic Potential: *İn Vitro* İnhibition Effects of Some Natural Phenolic Compounds On α-Glycosidase and α-Amylase Enzymes. *J. Biochem. Mol. Toxicol.* **2017**, *31*, 1–6. DOI: 10.1002/jbt.21956.

[8] Öztaşkın, N.; Kaya, R.; Maraş, A.; Şahin, E.; Gülcin, İ.; Göksu, S. Synthesis and Characterization of Novel Bromophenols: Determination of Their Anticholinergic, Antidiabetic and Antioxidant Activities. *Bioorg. Chem.* **2019**, *87*, 91–102. DOI: 10.1016/j.bioorg.2019.03.010.

[9] Worsztynowicz, P.; Napierała, M.; Białas, W.; Grajek, W.; Olkowicz, M. Pancreatic α-Amylase and Lipase İnhibitory Activity of Polyphenoliccompounds Present in the Extract of Black Chokeberry (*Aronia melanocarpa* L.). *Process Biochem.* **2014**, *49*, 1457–1463. DOI: 10.1016/j.procbio.2014.06.002.

[10] Menteşe, E.; Baltaş, N.; Bekircan, O. Synthesis and Kinetics Studies of *N′*-(2-(3,5-Disubstituted-4H-1,2,4-Triazol-4-yl)Acetyl)-6/7/8-Substituted-2-Oxo-2H-Chromen-3-Carbohydrazide Derivatives as Potent Antidiabetic Agents. *Arch. Pharm. Chem. Life. Sci.* **2019**, *352*, 1900227–1900227. DOI: 10.1002/ardp.201900227.

[11] Yakan, H. Preparation, Structure Elucidation, and Antioxidant Activity of New Bis(thiosemicarbazone) Derivatives. *Turk. J. Chem.* **2020**, *44*, 1085–1099. DOI: 10.3906/kim-2002-76.

[12] Lekshmi, K.; Sunitha, S.; Nath, R. Antioxidant, Antidiabetic and Anticancer Studies of Nickel Complex of Vanillin-4-Methyl-4-Phenyl-3-Thiosemicarbazone. *Mater. Today* **2021**, *41*, 669–675. DOI: 10.1016/j.matpr.2020.05.376.

[13] Missioui, M.; Mortada, S.; Guerrab, W.; Serdaroğlu, G.; Kaya, S.; Mague, J. T.; Essassi, E. M.; Faouzi, M. E. A.; Ramli, Y. Novel Antioxidant Quinoxaline Derivative: Synthesis, Crystal Structure, Theoretical Studies, Antidiabetic Activity and Molecular Docking Study. *J. Mol. Struct.* **2021**, *1239*, 130484–130411. DOI: 10.1016/j.molstruc.2021.130484.

[14] Shehzad, M. T.; Khan, A.; Islam, M.; Hameed, A.; Khiat, M.; Halim, S. A.; Anwar, M. U.; Shah, S. R.; Hussain, J.; Csuk, R.; et al. Synthesis and Urease İnhibitory Activity of 1,4-Benzodioxane-Based Thiosemicarbazones: Biochemical and Computational Approach. *J. Mol. Struct.* **2020**, *1209*, 127922–127928. DOI: 10.1016/j.molstruc.2020.127922.

[15] Zhang, X.; Qi, F.; Wang, S.; Song, J.; Huang, J. Synthesis, Structure, İn Silico ADME Evaluation and *İn Vitro* Antioxidant of (E)-*N*-(4-Ethylphenyl)-2-(İsomeric Methylbenzylidene) Thiosemicarbazone Derivatives. *J. Mol. Struct.* **2020**, *1199*, 126972–126979. DOI: 10.1016/j.molstruc.2019.126972.

[16] Nehar, O. K.; Mahboub, R.; Louhibi, S.; Roisnel, T.; Aissaoui, M. New Thiosemicarbazone Schiff Base Ligands: Synthesis, Characterization, Catecholase Study and Hemolytic Activity. *J. Mol. Struct.* **2020**, *1204*, 127566–127511. DOI: 10.1016/j.molstruc.2019.127566.

[17] Osmaniye, D.; Sağlık, B. N.; Levent, S.; et al. Design, Synthesis and Biological Evaluation of New n-Acyl Hydrazones with a Methyl Sulfonyl Moiety as Selective COX-2 İnhibitors. *Chem. Biodivers.* **2021**, *18*, 1–12. DOI: 10.1002/cbdv.202100521.

[18] Feng, S.; Li, C.; Chen, D.; Zheng, X.; Yun, H.; Gao, L.; Shen, H. C. Discovery of Methylsulfonyl İndazoles as Potent and Orally Active Respiratory Syncytial Virus (RSV) Fusion Inhibitors. *Eur. J. Med. Chem.* **2017**, *138*, 1147–1157. DOI: 10.1016/j.ejmech.2017.07.032.

[19] Gong, X.; Wang, M.; Ye, S.; Wu, J. Synthesis of 3-(Methylsulfonyl) Benzo[B]Thiophenes from Methyl(2-Alkynylphenyl)Sulfanes and Sodium Metabisulfite via A Radical Relay Strategy. *Org. Lett.* **2019**, *21*, 1156–1160. DOI: 10.1021/acs.orglett.9b00100.

[20] Apak, R.; Gorinstein, S.; Böhm, V.; Schaich, K. M.; Özyürek, M.; Güçlü, K. Methods of Measurement and Evaluation of Natural Antioxidant Capacity/Activity (IUPAC Technical Report). *Pure Appl. Chem.* **2013**, *85*, 957–998. DOI: 10.1351/PAC-REP-12-07-15.

[21] Daina, A.; Michielin, O.; Zoete, V. SwissADME: A Free Web Tool to Evaluate Pharmacokinetics, Drug-Likeness and Medicinal Chemistry Friendliness of Small Molecules. *Sci. Rep.* **2017**, *7*, 42717–42713. DOI: 10.1038/srep42717.

[22] Ribeiro, A. G.; Almeida, S. M. V. d.; de Oliveira, J. F.; Souza, T. R. C. d. L.; Santos, K. L. D.; Albuquerque, A. P. d.B.; Nogueira, M. C. d. B. L.; Carvalho Junior, L. B. d.; Moura, R. O. d..; da Silva, A. C.; et al. Novel 4-Quinoline-Thiosemicarbazone Derivatives: Synthesis, Antiproliferative Activity, *İn Vitro* and *İn Silico* Biomacromolecule İnteraction Studies and Topoisomerase İnhibition. *Eur. J. Med. Chem.* **2019**, *182*, 111592–111516. DOI: 10.1016/j.ejmech.2019.111592.

[23] Çavuşoğlu, B.; Sağlık, B.; Osmaniye, D.; Levent, S.; Acar Çevik, U.; Karaduman, A.; Özkay, Y.; Kaplancıklı, Z. Synthesis and Biological Evaluation of New Thiosemicarbazone Derivative Schiff Bases as Monoamine Oxidase İnhibitory Agents. *Molecules* **2017**, *23*, 60–18. DOI: 10.3390/molecules23010060.

[24] Apak, R.; Güçlü, K.; Ozyürek, M.; Karademir, S. E. Novel Total Antioxidant Capacity İndex for Dietary Polyphenols and Vitamins C and E, Using Their Cupric İon Reducing Capability in the Presence of Neocuproine: CUPRAC Method. *J. Agric. Food Chem.* **2004**, *52*, 7970–7981. DOI: 10.1021/jf048741x.

[25] Benzie, I. F. F.; Strain, J. J. Ferric Reducing/Antioxidant Power Assay: Directmeasure of Total Antioxidant Activity of Biological Fluids and Modified Versionfor Simultaneous Measurement of Total Antioxidant Power and Ascorbic Acid Concentration. *Methods Enzymol.* **1999**, *299*, 15–27. DOI: 10.1016/s0076-6879(99)99005-5[9916193.

[26] Baltas, N. Investigation of a Wild Pear Species (*Pyrus elaeagnifolia* subsp. *Elaeagnifolia* Pallas) from Antalya, Turkey: Polyphenol Oxidase Properties and Anti-Xanthine Oxidase, Anti-Urease, and Antioxidant Activity. *Int. J. Food Prop.* **2017**, *20*, 585–595. DOI: 10.1080/10942912.2016.1171777.

[27] Brand-Williams, W.; Cuvelier, M. E.; Berset, C. Use of a free-radical method to evaluate antioxidant activity. *LWT-Food Sci. Technol.* **1995**, *28*, 25–30. DOI: 10.1016/S0023-6438(95)80008-5.

[28] Özil, M.; Parlak, C.; Baltaş, N. A Simple and Efficient Synthesis of Benzimidazoles Containing Piperazine or Morpholine Skeleton at C-6 Position As Glucosidase İnhibitors with Antioxidant Activity. *Bioorg. Chem.* **2018**, *76*, 468–477. DOI: 10.1016/j.bioorg.2017.12.019.

[29] Baltaş, N. α-Glucosidase and α-Amylase İnhibition of Some Ethanolic Propolis Samples. *U. Bee J.* **2021**, *21*, 1–7. DOI: 10.31467/uluaricilik.877301.

[30] Lineweaver, H.; Burk, D. The Determination of Enzyme Dissociation Constant. *J. Am. Chem. Soc.* **1934**, *56*, 658–661. DOI: 10.1021/ja01318a036.

[31] Unnikrishnan, P. S.; Suthindhiran, K.; Jayasri, M. A. Alpha-Amylase İnhibition and Antioxidant Activity of Marine Green

Algae and its Possible Role in Diabetes Management. *Phcog. Mag.* **2015**, *11*, 511–515. DOI: 10.4103/0973-1296.172954.

[32] Morris, G. M.; Huey, R.; Lindstrom, W.; Sanner, M. F.; Belew, R. K.; Goodsell, D. S.; Olson, A. J. AutoDock4 and AutoDockTools4: Automated Docking with Selective Receptor Flexibility. *J. Comput. Chem.* **2009**, *30*, 2785–2791. DOI: 10.1002/jcc.21256.

[33] Ravindranath, P. A.; Forli, S.; Goodsell, D. S. AutoDockFR: Advances in Protein-Ligand Docking with Explicitly Specified Binding Site Flexibility. *PLOS Comput. Biol.* **2015**, *11*, 1–28. DOI: 10.1371/journal.pcbi.1004586.

[34] Dassault systèmes BIOVIA. Discovery Studio Modeling Environment. *Release 2020*. Dassault Systèmes: San Diego, **2020**.